Environ. Sci. Technol. **2007**, *41,* 1232−1237

Binding of Iron(III) to Organic Soils: EXAFS Spectroscopy and Chemical Equilibrium Modeling

JON PETTER GUSTAFSSON,*,[†]
INGMAR PERSSON,[‡]
DAN BERGGREN KLEJA,[§] AND
JORIS W. J. VAN SCHAIK[§]

Department of Land and Water Resources Engineering, Royal Institute of Technology, SE-100 44 Stockholm, Sweden; Department of Chemistry, Swedish University of Agricultural Sciences, Box 7015, SE-750 07 Uppsala, Sweden, and Department of Soil Sciences, Swedish University of Agricultural Sciences, Box 7014, SE-750 07 Uppsala, Sweden

The complexation of iron(III) to soil organic matter is important for the binding of trace metals in natural environments because of competition effects. In this study, we used extended X-ray absorption fine structure (EXAFS) spectroscopy to characterize the binding mode for iron(III) in two soil samples from organic mor layers, one of which was also treated with iron(III). In most cases the EXAFS spectra had three significant contributions, inner-core Fe−O/N interactions at about 2.02(2) Å, Fe−C interactions in the second scattering shell at 3.00(4) Å, and a mean Fe−Fe distance at 3.37(3) Å. One untreated sample showed features typical for iron (hydr)oxides; however, after treatment of iron(III) the EXAFS spectrum was dominated by organically complexed iron. The presence of a Fe−Fe distance in all samples showed that the major part of the organically complexed iron was hydrolyzed, most likely in a mixture of complexes with an inner core of $(O_5Fe)_2O$ and $(O_5Fe)_3O$. These results were used to constrain a model for metal−humic complexation, the Stockholm Humic Model (SHM). The model was able to describe iron(III) binding very well at low pH considering only one dimeric iron(III)−humic complex. The competition effect on trace metals was also well described.

Introduction

Despite its common occurrence, the mechanisms governing the interactions between iron(III) and natural organic matter are not clear. Recently, Tipping et al. (*1*) highlighted the importance iron(III) may have on the binding of trace metals to organic matter. Due to the strong binding of iron(III) to carboxylate and phenolate groups, iron(III) is expected to compete strongly for complexation sites. However, the chemistry of the Fe-organic interaction is still unclear, particularly concerning the possible role of iron redox reactions. For example, Pullin and Cabaniss (*2*), using a kinetic analysis method, found that both iron(II)- and iron(III)-fulvic acid complexes were important iron species in the natural waters they investigated. Conversely, Steinmann and Shotyk (*3*, *4*) found evidence for the predominant role of iron(III)−humic acid complexes in pore waters from peats. These authors hypothesized that the iron(III) oxidation state was important due to the much stronger affinity of iron(III) than of iron(II) to humic acid functional groups.

For a number of years, X-ray absorption fine-structure spectroscopy (XAFS) has been important in unraveling the coordination modes of ions to ligands and particle surfaces in soils and waters (*5*, *6*). Rapid advances in these techniques now permit structural analysis of organic matter complexes. For example, cadmium(II) binding to mor layers was recently investigated with extended X-ray absorption fine structure spectroscopy (EXAFS) and was found to involve −SH groups with the organic matter (*7*).

Information from spectroscopic studies can be used to constrain geochemical models. In particular, models for metal complexation can be improved by considering the actual coordination environment of the formed metal−ligand complex (*8*). This should lead to better simulations of metal binding and competition effects in soils. In this work we have applied EXAFS to study the coordination mode of iron in two organic soils. Our objective was to investigate whether the EXAFS evidence could be used to constrain a geochemical model for metal−humic complexation, the Stockholm Humic Model (SHM) (*9*−*11*), and whether the model was able to describe the competitive effect of the binding of iron(III) on selected trace metals.

Materials and Methods

Soils. In this work we used three mor layers (Oe horizons) from Swedish Spodosols. All three were similar as regards the extent of decomposition, although they contained slightly different concentrations of extractable iron (Table S1, Supporting Information). The samples were used in their field-moist state. Untreated field-moist samples from Asa Oe and Risbergshöjden Oe, and iron(III)-enriched samples from Risbergshöjden Oe, were used for the EXAFS study. The latter samples were prepared by mixing 20 g field-moist soil with a 600 cm^3 solution consisting of 1.5 $mmol\cdot dm^{-3}$ $Fe(NO_3)_3$ + 5.5 $mmol\cdot dm^{-3}$ $NaNO_3$. This addition corresponds to 140 mmol Fe(III) per kg dry matter. These suspensions were shaken for one week. After centrifugation, the supernatant was discarded. Samples were subjected to EXAFS analysis after 2 days, although an additional sample was stored for 10 days (at 281 K) before analysis. The pH of the samples was 3.8 (Asa Oe), 3.9 (untreated Risbergshöjden Oe), and 2.6 (iron(III)-enriched Risbergshöjden Oe). To provide references for the EXAFS analysis, ferrihydrite and goethite were synthesized (*12*).

EXAFS. Iron K edge X-ray absorption spectra were recorded at the bending magnet beam-line 2−3 at Stanford Synchrotron Radiation Laboratory (SSRL), U.S., equipped with a Si [220] double crystal monochromator, the storage ring operated at 3.0 GeV and a maximum current of 100 mA (*13*), and at beam-line I811 at MAX-lab, Lund University, Sweden, equipped with a Si[111] double crystal monochromator, the storage ring operated at 1.5 GeV and a maximum current of 200 mA (*14*). Data collection was performed in fluorescence mode using a Lytle detector with manganese filter for all samples. In order to remove higher-order harmonics, the beam intensity was detuned to 40% of the maximum intensity at the end of the scans. The soil samples were kept in a 1.5 mm thick silver frame with 6.3 μm X-ray polypropylene foil windows. The energy calibration of the

---

* Corresponding author phone: +46 8 790 8316; fax: +46 8 411 0775; e-mail: gustafjp@kth.se.

[†] KTH (Royal Institute of Technology).

[‡] Department of Chemistry, Swedish University of Agricultural Sciences.

[§] Department of Soil Sciences, Swedish University of Agricultural Sciences.

10.1021/es0615730 CCC: $37.00

X-ray absorption spectra were performed by simultaneously recording the spectrum of a metallic iron foil, and assigning the first K-edge inflection point to 7111.3 eV (*15*). Four scans were recorded for each sample, and the EXAFSPAK program package was used for energy calibration and averaging (*16*).

The EXAFS data analysis was performed with the GNXAS code using previously developed and widely applied methods (*17*, *18*). In the GNXAS approach the interpretation of the experimental data is based on the decomposition of the EXAFS $\chi(k)$ signal, defined as the oscillation with respect to the atomic background cross-section normalized to the corresponding K-edge channel cross-section (*17*), into a summation over n-body distribution functions $\gamma^{(n)}$ calculated by means of the multiple-scattering (MS) theory. Each signal has been calculated in the muffin-tin approximation using the Hedin−Lundqvist energy dependent exchange and correlation potential model, which includes inelastic loss effects (*19*).

Batch Experiments. In batch experiments, 1.00 g field-moist soil was suspended in 30 mL solutions of variable composition in polypropylene centrifuge tubes and then shaken for 7 days in a shaking-water bath at 281 K and at a background ionic strength of 0.01 mol·dm^{-3} ($NaNO_3$ was used as supporting electrolyte). Procedures for filtration, pH measurement, and analyses of metals and major solutes have been described fully in an earlier paper (*10*). The Korsmossen Oe sample was investigated for its iron-binding properties at low pH. This was accomplished by shaking duplicate samples with 0, 0.2, and 0.5 mmol·dm^{-3} $Fe(NO_3)_3$ and with different additions of acid (as nitric acid) to generate pH values in the range from 2.3 to 4. The Risbergshöjden Oe samples were equilibrated with 0.02 mmol·dm^{-3} $Cd(NO_3)_2$, 0.02 mmol·dm^{-3} $Ni(NO_3)_2$, 0.02 mmol·dm^{-3} $Co(NO_3)_2$, and 0.05 mmol·dm^{-3} $VOSO_4$ to quantify the sorption of these trace metals at different pH values; the metals were added together. The binding of these trace metals was studied in the absence and presence of iron and aluminum as 1.5 mmol·dm^{-3} $Fe(NO_3)_3$ or 1.5 mmol·dm^{-3} $Al(NO_3)_3$, respectively. For Fe(III) the addition was identical to the one used for the EXAFS study (140 mmol Fe per kg dry matter), which made it possible to link the observed concentrations of dissolved Fe(III) and trace metals to the EXAFS results on Fe(III) binding.

Equilibrium Modeling. The Visual MINTEQ software was used (*20*), which contains the SHM model as recently revised for soil suspensions (*11*). Solution speciation was calculated using thermodynamic data of the Visual MINTEQ database, which mostly relies on the NIST Critical Stability constants database (*21*). We used the Davies equation for activity correction. Details on the equations used for metal complexation in the SHM are found in the Supporting Information.

Model Application. For the soil suspensions, we assumed that 75% of the "active" solid-phase organic matter consisted of humic acid (HA), whereas 25% was fulvic acid (FA) (*11*). Furthermore, we assumed that 100% of the dissolved organic matter in these suspensions was FA. To consider the effect of initially bound metals in the modeling, the input for "active" aluminum, iron, and trace metals was estimated from extraction with 0.1 mol·dm^{-3} nitric acid. For the total concentrations of calcium and magnesium we used the barium(II) chloride-extractable values (see Table S1, Supporting Information). For sodium and nitrate, the total concentrations were calculated from the added amounts considering also the initial amount of sodium as extracted by barium(II) chloride. Finally, total potassium and manganese were estimated from the maximum amount dissolved at low pH (*10*).

For the proton binding parameters, we used the generic values for the SHM as reported by Gustafsson and van Schaik (*10*). For the soil suspensions from Risbergshöjden and Korsmossen, modeling was done in four steps: (1) From the observed buffer curve, we optimized the fraction of the total organic matter that was "active" with respect to cation binding (f_{HS-tot}), through the comparison of measured and simulated pH values for a given addition of acid or base (*10*). The f_{HS-tot} parameter determines the slope of the modeled buffer curve. (2) Complexation constants for iron(III) and aluminum(III) were adjusted to provide an optimum fit to observed concentrations of dissolved iron(III) and aluminum(III). (3) For the data set from Risbergshöjden Oe, cation complexation constants for cadmium(II), cobalt(II), nickel(II), and vanadyl(IV) were optimized for samples for which no additions of iron(III) and aluminum(III) had been made. (4) Finally for the Risbergshöjden Oe data, the effect of iron(III) and aluminum(III) competition on trace metal binding was predicted.

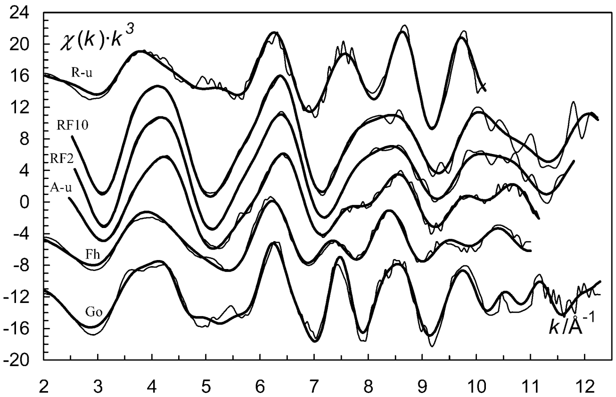

FIGURE 1. Stacked, normalized k^3-weighted EXAFS spectra for Fe in the untreated Asa Oe sample (A-u, no offset), in Risbergshöjden Oe with added iron(III) analyzed 2 days (RF2, offset +4.0) and 10 days (RF10, offset +8.0) after the end of the batch experiment, and in the untreated Risbergshöjden Oe sample (R-u, offset 16.0). The spectra for synthetic ferrihydrite (Fh, offset −4.0) and goethite (Go, offset −12.0) are given for comparison. Thin and thick lines represent the normalized data and best fits, respectively.

Results

EXAFS. The untreated Oe samples from Risbergshöjden and Asa showed slightly different EXAFS spectra. For the untreated Risbergshöjden Oe sample, the large amplitude at high k values showed the presence of several Fe−Fe distances. The Fe−O/N bond distance at 2.00(2) Å (it is not possible with the EXAFS technique to distinguish between O and N) showed that the iron was present in the oxidation state +III. A strong and well-defined Fe−Fe distance at 3.00(2) Å showed the presence of one or several iron(III) (hydr)oxide minerals such as ferrihydrite, goethite and akaganeite; the iron EXAFS spectrum of the untreated soil had close similarities with that of goethite, see Figure 1. The other refined Fe−Fe distance at 3.38(3) Å can be related to Fe−Fe distances in either $(FeO_5)_2O$ and $(FeO_5)_3O$ complexes (see below) and/or in any iron(III) (hydr)oxide mineral. There was also a significant distance to iron from a heavy back-scatterer such as lead at 3.73(3) Å (Table 1). The EXAFS spectra are shown in Figure 1 (see also Figure S1, Supporting Information). The Fe−O bond distance in our goethite and ferrihydrite samples was 1.98(2) and 1.96(2) Å, respectively. The Fe−Fe distances in goethite were 3.00(2), 3.26(2), 3.44(3), 4.64(3), 4.88(4), and 5.45(4) Å; in ferrihydrite they were 3.03(2) and 3.44(3) Å.

The EXAFS spectra of the samples from the untreated Asa Oe sample had a significantly higher iron content and three contributions, inner-core Fe−O/N interactions at 2.02(2) Å, Fe−C interactions in the second scattering shell at 3.00(4) Å, and a Fe−Fe distance at 3.37(3) Å could be identified (Figure 1). Again the mean Fe−O/N bond distance shows that iron

TABLE 1. Summary of Structure Parameters, Distances, d/Å, Debye−Waller Factor Coefficient, σ^2/Å^2, and Number of Distances, N, from the Refinements of the Iron K Edge EXAFS Data (The Number of Distances has been Fixed)

sample	interaction	d/Å	σ^2/Å^2	N
Asa Oe, untreated	Fe−O	1.88(2)	0.0030(2)	1
	Fe−O	2.00(2)	0.0075(2)	5
	Fe−Fe	3.38(3)	0.004(1)	1
	Fe−C	3.02(4)	0.008(2)	5
Risbergshöjden Oe, untreated	Fe−O	2.00(2)	0.008(3)	6
	Fe−Fe	3.01(2)	0.004(1)	2
	Fe−Fe	3.38(2)	0.004(1)	1
	Fe−Pb	3.72(3)	0.004(1)	2
Risbergshöjden Oe with Fe, 2 days	Fe−O	1.88(2)	0.0050(3)	1
	Fe−O	2.03(2)	0.0085(4)	5
	Fe−Fe	3.37(2)	0.005(1)	1
	Fe−C	3.00(3)	0.010(3)	5
Risbergshöjden Oe with Fe, 10 days	Fe−O	1.86(2)	0.0022(3)	1
	Fe−O	2.02(2)	0.0078(4)	5
	Fe−Fe	3.34(2)	0.012(1)	1
	Fe−C	3.00(3)	0.009(2)	5

was present as iron(III), and that the iron(III) had an octahedral configuration; corresponding iron(II) bond distances are ca. 0.10 Å longer (*22−24*). The Debye−Waller coefficient was larger than normally found for this type of octahedral iron(III) structures (*22*) indicating that the bond distance distribution was much wider than normal. The presence of a second shell of back-scatterers at 3.0 Å showed that that organic groups, e.g., phenolate and carboxylate, were bound to iron(III) at expected distances and angles. The presence of a Fe−Fe distance showed unambiguously that the dominating iron species in Asa Oe was hydrolyzed. The observed Fe−Fe distance strongly indicates that this hydrolyzed species contained a mixture of dimers and trimers with one and three μ-oxo bridges between the iron(III) ions, respectively, whereas complexes with a double hydroxo bridge can more or less be excluded as the Fe−Fe distance in such complexes is much shorter, 2.9−3.2 Å (*23*, *24*). The Fe−Fe distance in $O_5Fe{-}O{-}FeO_5$ complexes is in the range of 3.44−3.56 Å depending on the Fe−O−Fe angles, which varies in the range 146−180° in the reported structures; the mean Fe−O_{oxo} bond distance is 1.79 Å (*23*, *24*), while in the trimers, a central oxide ion binds to three iron(III) ions, and the mean Fe−O_{oxo} bond and Fe−Fe distances are 1.90 and ca. 3.35 Å, respectively (*23*, *24*). With this result in hand, a model with one Fe−O bond distance significantly shorter than the remaining five was introduced, and the fit of the experimental data did improve. The short Fe−O_{oxo} bond distance was refined to 1.85(2) Å, whereas the mean Fe−O bond distance of the remaining five bonds is 2.02(2) Å (Table 1). The Debye−Waller factor coefficients of the short Fe−O and the Fe−Fe distances were also somewhat larger than expected for only one type of complex present with normal bond distance distribution supporting that there was a mixture of $(O_5Fe)_3O$ and $(O_5Fe)_2O$ complexes in the sample.

In the literature, a large number of crystal structures of $(O_5Fe)_2O$ and $(O_5Fe)_3O$ complexes have been reported. The $(O_5Fe)_2O$ complexes display an almost linear Fe−O−Fe entity as seen in both the hydrated, $[(H_2O)_5Fe{-}O{-}Fe(OH_2)_5]^{4+}$ (*25*, *26*), and complexed form, $(O/N)_5{-}Fe{-}O{-}Fe(O/N)_5$ (*27−31*). The $(O_5Fe)_3O$ complexes consist normally of at least six bidentate oxygen donor ligands, while the iron(III) binds water or any other monodentate ligand in the sixth position (*23*). See Table S2, Supporting Information, for more references on $(O_5Fe)_2O$ structures.

The EXAFS spectra of the Risbergshöjden Oe samples, to which iron(III) had been added, were identical to those of the untreated Asa Oe sample (Figure 1). Thus the dominating reactive iron species in these organic soils appeared to be hydrolyzed dimeric and trimeric iron(III) complexes where the iron(III) ions are connected by a μ-oxo bridge. The time required to hydrolyze the iron(III)−organic matter complexes seemed to be less than 1 week (i.e., the duration of the batch experiment), and no further changes occurred on storage for an additional week before analysis.

The EXAFS results were incompatible with the usual way metal−humic complexes are treated in today's equilibrium models. For example, in WHAM 6 (*32*), iron(III)−humic complexes are assumed to consist of monomeric Fe, which can be coordinated in monodentate, bidentate, or tridentate configurations. The same was true for the original version of SHM.

Results from Batch Experiments and Modeling for Soil Systems. The experimental results for dissolved iron of the Risbergshöjden Oe and Korsmossen Oe suspensions are shown in Figure 2. To the Korsmossen Oe suspension, comparably low iron additions were made (0.2 and 0.5 mmol·dm^{-3} iron(III)). Under these conditions, iron(III) was very strongly bound, with between 98 and 99% sorbed even at pH 2.3. Larger additions of iron were made to the Risbergshöjden Oe suspension (1.5 mmol·dm^{-3} iron(III)). The sorption of iron(III) was now 89% at pH 2.3, but already at pH 2.9 the sorption percentage had increased to >98%. At

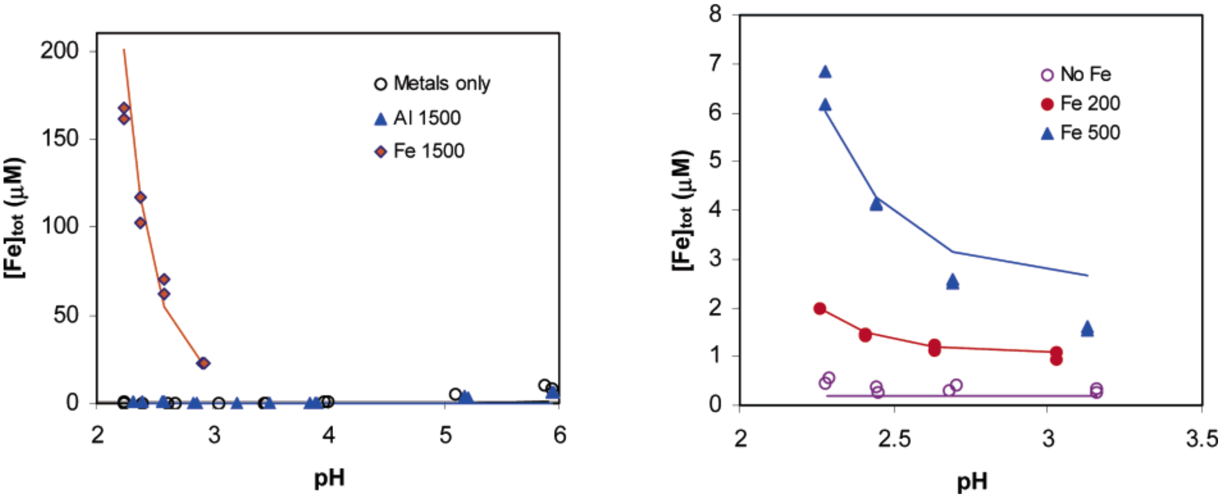

FIGURE 2. Total dissolved Fe, $[Fe]_{tot}$, against pH for Risbergshöjden Oe (left) and Korsmossen Oe (right). Titrations of soil samples with HNO_3 and NaOH, with and without the addition of $Fe(NO_3)_3$ or $Al(NO_3)_3$ (see text for details). The points are observed values. The lines are model fits.

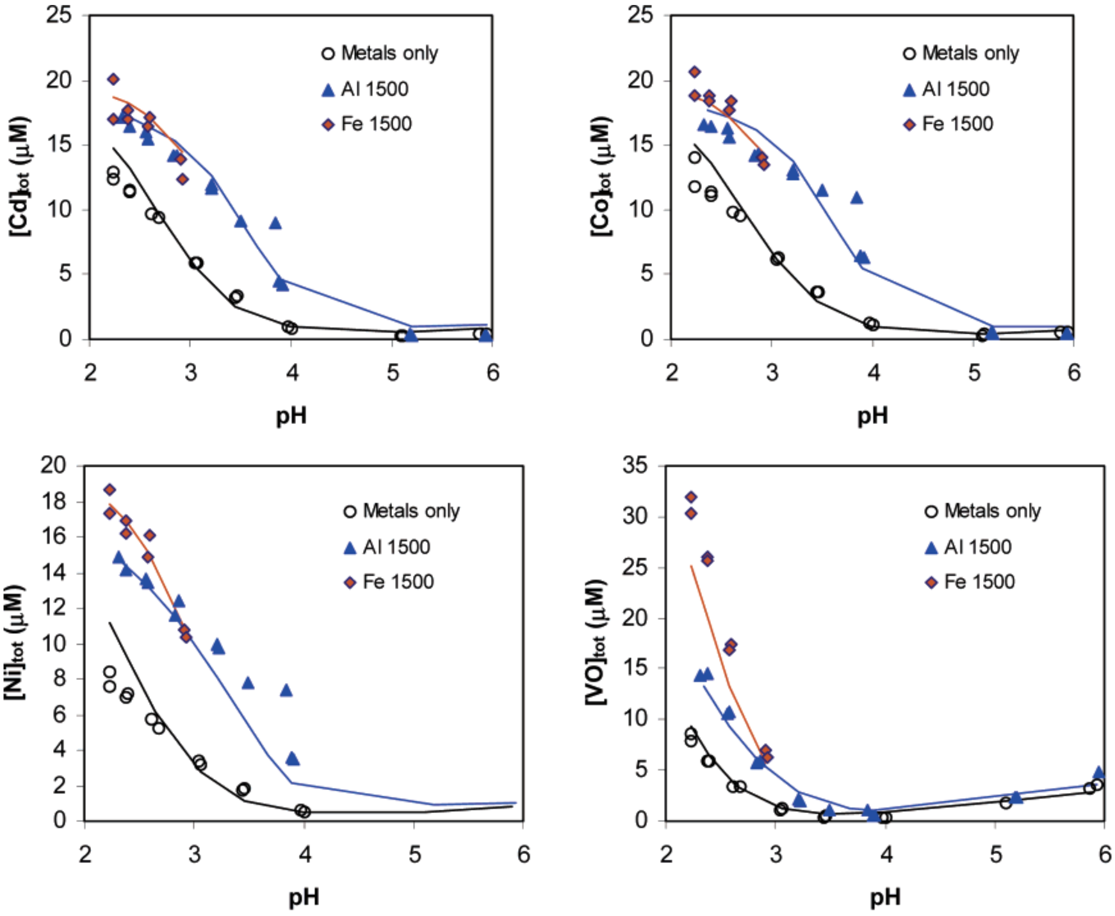

FIGURE 3. Total dissolved Cd, Co, Ni and VO against pH for Risbergshöjden Oe. Titrations of soil samples with HNO_3 and NaOH, with and without the addition of $Fe(NO_3)_3$ or $Al(NO_3)_3$ (see text for details). The points are observed values. The lines are model fits.

pH < 3, the slope for dissolved iron(III) vs pH was simulated most successfully with the SHM when a proton exchange stoichiometry of five protons per two atoms of complexed iron(III) was used. Together with the EXAFS results, this observation was used to constrain a model description for Fe−organic complexation in the SHM. A simple change in the Visual MINTEQ code allowed for the inclusion of the following reaction in SHM:

$$3R\mathrm{OH} + 2\mathrm{Fe}^{3+} + \mathrm{H_2O} \rightleftharpoons (R\mathrm{O})_3\mathrm{Fe_2O}^{+} + 5\ \mathrm{H}^{+}\ K_{\mathrm{Fe,t}} \quad (1)$$

where $K_{\mathrm{Fe,t}}$ is a complexation constant that considers also electrostatic contributions (Table S4, Supporting Information). According to the model, iron(III) forms a dimer (Fe_2O^{4+}), which reacts with three carboxylate or phenolate functional groups to form a complex. This is in better agreement with the EXAFS results, although the latter indicate that trimers are also involved (however, the inclusion of trimeric complexes would increase the degrees of freedom of the model). The assumed relative contribution of carboxylate and phenolate sites to iron(III) complexation is shown in the Supporting Information (Table S3). It was found that all data from the soil suspensions were described well using a single dimeric $(RO)_3Fe_2O^+$ complex with log $K_{\mathrm{Fe,t}} = -5.15$ and $\Delta LK_2 = 1.8$.

Trace metal binding decreased after addition of 1.5 mM iron(III) or aluminum(III) (Figure 3). Again when using a single $(RO)_3Fe_2O^+$ complex for iron(III) binding, we were able to simulate the competition from iron(III) very well considering the simplicity of the model. Model simulations suggest that iron(III) is a stronger competitor with trace metals than aluminum(III). This is partly due to the stronger overall binding of iron(III). At pH 2.3, only about 32% of the active aluminum was sorbed after addition of 1.5 mmol·dm^{-3} aluminum(III), compared with 89% for iron(III). Furthermore, iron(III) is bound more strongly to the high-affinity sites, as evidenced by the ΔLK_2 value of 1.8 for iron(III) and 1 for aluminum(III); this makes iron(III) a more potent competitor for trace metals such as nickel(II) and cadmium(II), which have a large degree of heterogeneous binding affinity. This is in line with the conclusions of Tipping et al. (*1*).

Testing the Model on Data from the Literature. The approach was also tested on a previously published data set for iron(III) binding to humic acid in the presence of ferrihydrite (*33*), using the iron hydrolysis constants for this system as interpreted by Milne et al. (*34*). For this system, the model derived for the mor layer led to overestimations of the total dissolved iron(III) concentration (Figure 4). However, after adjustment of the ΔLK_2 value from 1.8 to 1.5, it was found that the model simulated the total dissolved iron(III) concentrations rather well both across the pH range (with a HA concentration of 0.6 ppm) and at pH 8 with different HA concentrations.

The competitive effect of iron(III) on Cu^{2+} complexation to humic acid was reported by Tipping and co-workers (*1*). In this case the model with the dimeric Fe complex was not able to fit the data well, particularly not at low Cu^{2+} activities (Figure 5). Much better fits were obtained with a combination of two monomeric iron(III) complexes (data not shown). Possibly, the short equilibration time used in this experiment (1 h, as compared to 1 week in the other experiments mentioned) may not have allowed sufficient formation of dimeric iron(III) species.

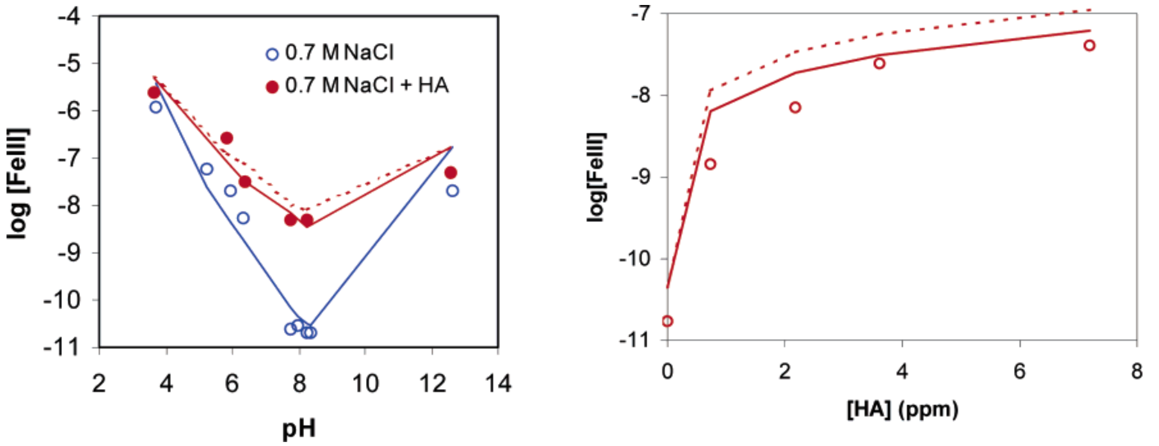

FIGURE 4. The concentration of dissolved iron(III) in systems with ferrihydrite and different amounts of humic acid. The points are the observations of Liu and Millero (1999). The lines are model fits with Visual MINTEQ using a log $^*K_s$ for ferrihydrite of 3.2 at 25 °C. Red dotted lines represent model fits with ΔLK_2 set to 1.8, whereas the red solid lines are model fits with $\Delta LK_2 = 1.5$ (see text).

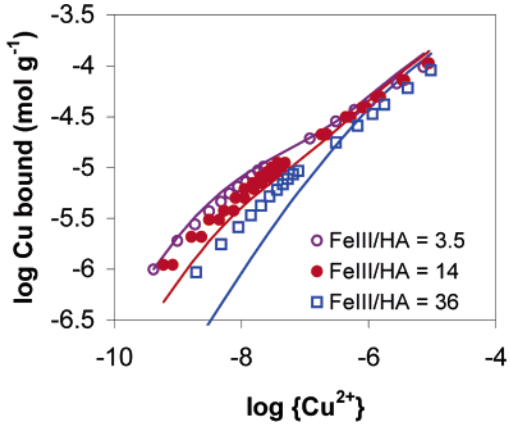

FIGURE 5. Copper complexation to 1 g/L humic acid at pH 4 and at different total concentrations of iron(III). Points are observations of Tipping et al. (*1*), and model fits with $\Delta LK_2 = 1.5$ for Fe(III) complexation. Copper complexation constants were set to: log $K[\mathrm{ROCu}^+] = -1.5$, log $K[(R\mathrm{O})_2\mathrm{Cu}] = -6.2$, and $\Delta LK_2 = 1.55$.

Discussion

The Structure of the Iron(III)−Organic Complex in Soil. The presence of a μ-oxo bridge between the iron(III) ions shows that the iron(III)−organic complexes, under aerobic and acid conditions in soil, are hydrolyzed. This is not surprising as very stable iron(III) complexes are required to resist hydrolysis. In addition, iron in the oxidation state +III is very much stabilized over the oxidation state +II in the presence of ligands binding through one or several phenolate groups (*35*), whereas other ligands as, e.g., phenantrolines and bipyridines stabilize iron(II) over iron(III) (*36*). The hydrolyzed iron(III)−organic complex is most probably stable enough to be the dominating species also in aerobic aqueous solutions.

Implications for the Understanding of Trace Metal Binding in Soils. The use of EXAFS evidence to constrain the SHM as regards iron(III) binding produced a model that was simple (with only a single complex) yet effective in describing both iron(III) complexation and its competitive effects on other trace metals. Moreover, the results show that iron(III) is a potent competitor and that it needs to be considered in simulations of trace metal binding in soils.

An unresolved problem when using the model for simulations is how to estimate the geochemically active concentration of iron(III) in soils. In this study we used 0.1 mol·dm^{-3} nitric acid to estimate this property, in line with earlier research (*1*). This is almost certainly an underestimation. With the SHM it can be estimated that between 30 and 40% of the organically complexed iron(III) will be desorbed at pH 1 (the results are valid for the Risbergshöjden Oe horizon, without extra iron(III) additions). On one hand, a more aggressive extractant will cause a better recovery, but on the other hand other, inorganic iron(III) phases, such as iron (hydr)oxides, may be dissolved. In addition, the kinetics of iron(III) release from organic complexes may be rather slow with many extractants, as has been shown for aluminum(III) (*37*).

Acknowledgments

This study was funded by the Swedish Research Council (VR). We acknowledge Niklas Ekberg, Jeanette Liedholm, Daniel Nordberg, Maria Stenström, and Erik Wall, who sampled the Risbergshöjden Oe soil and who conducted many of the batch equilibrations with this soil. Nathalie Camatte sampled the Korsmossen Oe soil. We acknowledge Stanford Synchrotron Radiation Laboratory (SSRL) and MAX-lab, Lund University for the allocation of beam time and laboratory facilities. SSRL is a national user facility operated by Stanford University on behalf of the U.S. Department of Energy, Office of Basic Energy Sciences. The SSRL Structural Molecular Biology Program is supported by the Department of Energy, Office of Biological and Environmental Research, and by the National Institutes of Health, National Center for Research Resources, Biomedical Technology Program. MAX-lab is supported by the Swedish Research Council and by The Knut and Alice Wallenberg Foundation, with additional support from The Crafoord Foundation and The Faculty of Science and Technology, Norwegian University of Science & Technology.

Supporting Information Available

Description of complexation reactions in the SHM, Characteristics of soil samples (Table S1), Crystal structures containing $(\mathrm{O_5Fe})_3\mathrm{O}$ entities (Table S2), Proton sites involved in tridentate complexes (Table S3), Table of species for SHM complexation reactions (Table S4), Input data for the SHM for the batch experiment suspensions (Table S5), Fourier Transforms of EXAFS data (Figure S1). This material is available free of charge via the Internet at http://pubs.acs.org.

Literature Cited

(1) Tipping, E.; Rey-Castro, C.; Bryan, S. E.; Hamilton-Taylor, J. Al(III) and Fe(III) binding by humic substances in freshwaters, and implications for trace metal speciation. *Geochim. Cosmochim. Acta* **2002**, *66*, 3211−3224.

(2) Pullin, M. J.; Cabaniss, S. E. The effect of pH, ionic strength, and iron-fulvic acid interactions on the kinetics of non-photochemical iron transformations. II. The kinetics of thermal reduction. *Geochim. Cosmochim. Acta* **2003**, *67,* 4079–4089.

(3) Steinmann, P.; Shotyk, W. Ion chromatography of organic-rich natural waters from peatlands. V. Fe^{2+} and Fe^{3+}. *J. Chromatogr. A* **1995**, *706,* 293–299.

(4) Steinmann, P.; Shotyk, W. Chemical composition, pH and redox state of sulfur and iron in complete vertical porewater profiles from two *Sphagnum* peat bogs, Jura Mountains, Switzerland. *Geochim. Cosmochim. Acta* **1997**, *61,* 1143–1163.

(5) Brown, G. E.; Sturchio, N. C. An overview of synchrotron radiation applications to low temperature geochemistry and environmental science. *Rev. Mineral. Geochem.* **2002**, *49,* 1–115.

(6) McNear, D. H.; Tappero, R.; Sparks, D. L. Shining light on metals in the environment. *Elements* **2005**, *1,* 67–70.

(7) Karlsson, T.; Persson, P.; Skyllberg, U. Extended X-ray absorption fine structure spectroscopy evidence for the complexation of cadmium by reduced sulfur groups in natural organic matter. *Environ. Sci. Technol.* **2005**, *39,* 3048–3055.

(8) Peacock, C. L.; Sherman, D. L. Copper(II) sorption onto goethite, hematite and lepidocrocite: a surface complexation model based on ab initio molecular geometries and EXAFS spectroscopy. *Geochim. Cosmochim. Acta* **2004**, *68,* 2623–2637.

(9) Gustafsson, J. P. Modeling the acid-base properties and metal complexation of humic substances with the Stockholm Humic Model. *J. Colloid Interface Sci.* **2001**, *244,* 102–112.

(10) Gustafsson, J. P.; van Schaik, J. W. J. Cation binding in a mor layer: batch experiments and modeling. *Eur. J. Soil Sci.* **2003**, *54,* 295–310.

(11) Gustafsson, J. P.; Berggren Kleja, D. Modeling salt-dependent proton binding by organic soils with the NICA-Donnan and Stockholm Humic models. *Environ. Sci. Technol.* **2005**, *39,* 5372–5377.

(12) Schwertmann, U.; Cornell, R. M. *Iron Oxides in the Laboratory. Preparation and Characterization*; Wiley: Weinheim, 2000.

(13) Dunn, L.; Tompkins, H. http://www-ssrl.slac.stanford.edu/beamlines/bl4–1./bl4–1.html.

(14) Carlson, S. Materials Science Beamline, I811, http://maxsun5.maxlab.lu.se/beamlines/bli811/.

(15) Thompson, A.; Attwood, D.; Gullikson, E.; Howells, M.; Kim, K.-J.; Kirz, J.; Kortright, J.; Lindau, I.; Pianatta, P.; Robinson, A.; Scofield, J.; Underwood, J.; Vaughan, D.; Williams, G.; Winick, H. *X-ray Data Booklet, LBNL/PUB-490 Rev. 2*; Lawrence Berkeley National Laboratory: Berkeley, CA, 94720, 2001.

(16) George, G. N.; Pickering, I. J. *EXAFSPAK—A Suite of Computer Programs for EXAFS Analysis*; SSRL, Stanford University, CA, 1993.

(17) Filipponi, A.; Di Cicco, A. X-ray absorption spectroscopy and n-body distribution functions in condensed matter. 2. Data analysis and applications. *Phys. Rev. B* **1995**, *52,* 15135–15149.

(18) Filipponi, A.; Di Cicco, A.; Natoli, C. R. X-ray absorption spectroscopy and n-body distribution functions in condensed matter. 1. Theory. *Phys. Rev. B* **1995**, *52,* 15122–15134.

(19) Sayers, D. E.; Bunker, B. A. In *X-ray absorption: Principles, Applications, Techniques of EXAFS, SEXAFS and XANES*, chapter 6; Koningsberger, D. C., Prins, R., Eds.: Wiley-Interscience: New York, 1988.

(20) Gustafsson, J. P. Visual MINTEQ version 2.50. http://www.lwr.kth.se/English/OurSoftware/vminteq/index.htm. Stockholm, Sweden, June 2006.

(21) Smith, R. M.; Martell, A. E.; Motekaitis, R. J. *NIST Critically Selected Stability Constants of Metal Complexes Database. Version 7.0*, NIST Standard Reference Database 46; National Institute of Standards and Technology, U.S. Department of Commerce: Gaithersburg, MD, 2003.

(22) D'Angelo, P.; Benfatto, M. Effect of multielectronic configurations on the XAFS analysis at the Fe K edge. *J. Phys. Chem. A* **2004**, *108,* 4505–4514.

(23) Allen, F. H.; Bellard, S.; Brice, M. D.; Cartwright, B. A.; Doubleday: A.; Higgs, H.; Hummelink, T.; Hummelink-Peters, C. G.; Kennard, O.; Motherwell, W. D. S.; Rodgers, J. R.; Watson, D. G. The Cambridge Crystallographic Data Centre: computer-based search, retrieval, analysis and display of information. *Acta Crystallogr. Sect. B* **1979**, *35,* 2331–2339, and references therein.

(24) Inorganic Crystal Structure Data Base, National Institute of Standards and Technology, Fachinformationszentrum, Karlsruhe, Release 05/1.

(25) Junk, P. C.; McCool, B. J.; Moubaraki, B.; Murray, K. S.; Spiccia, L. Supramolecular complexation and polynuclear aqua ions: A crown ether adduct of a μ-oxo bridged iron(III) aqua dimer. *Angew. Chem. Int. Ed.* **1999**, *38,* 2224–2226.

(26) Junk, P. C.; McCool, B. J.; Moubaraki, B.; Murray, K. S.; Spiccia, L.; Cashion, J. D.; Steed, J. W. Utilization of crown ethers to stabilize the dinuclear μ-oxo bridged iron(III) aqua ion, $[(H_2O)_5Fe(\mu\text{-}O)Fe(H_2O)_5]^{4+}$. *J. Chem. Soc. Dalton Trans.* **2002**, 1024–1029.

(27) Taft, K. L.; Masschelein, A.; Shuncheng Lui Lippard, S. J.; Garfinkel-Shweky, D.; Bino, A. Models of the oxidized forms of polyiron oxo proteins: Synthetic routes to (μ-oxo)bis(μ-carboxylato)diiron(III) complexes with neutral monodentate and bidentate capping ligands. *Inorg. Chim. Acta* **1992**, *198,* 627–631.

(28) Ahlers, C.; Dickman, M. H. Iron mediated cleavage of coordinated 1, 1,1,5,5,5-hexafluoropentane-2,4-dione by the 2,2,6,6-tetramethylpiperidine-1-oxyl nitroxyl radical. *Inorg. Chem.* **1998**, *37,* 6337–6340.

(29) The Cambridge Crystallographic Data Centre, code no. KONGOJ, Barium (μ_2-oxo)bis(aqua-(nitrilotriacetato)-iron(III)) tetrahydrate.

(30) Villamena, F. A.; Dickman, M. H.; Crist, D. R. Nitrones as ligands in complexes of Cu(II), Mn(II), Co(II), Ni(II), Fe(II), and Fe(III) with N-*tert*-Butyl-α-(2-pyridyl)nitrone and 2,5,5-trimethyl-1-pyrroline-N-oxide. *Inorg. Chem.* **1998**, *37,* 1446–1453.

(31) Ou, C. C.; Wollmann, C. G.; Hendrickson, D. N.; Potenza, J. A.; Schugar, H. J. Molecular structure and magnetic properties of (μ-oxo)bis[4-chloro-2,6-pyridinecarboxylatodiaquairon(III)] tetrahydrate, $[Cl\text{-}C_7H_2NO_4(H_2O)_2Fe]_2O\cdot H_2O$, complex with linear $Fe_2O_4^+$ unit. *J. Am. Chem. Soc.* **1978**, *100,* 4717–4724.

(32) Tipping, E. Humic ion-binding model VI: An improved description of the interactions of protons and metal ions with humic substances. *Aquat. Geochem.* **1998**, *4,* 3–47.

(33) Liu, X.; Millero, F. J. The solubility of iron hydroxide in sodium chloride solutions. *Geochim. Cosmochim. Acta* **1999**, *63,* 3487–3497.

(34) Milne, C. J.; Kinniburgh, D. G.; van Riemsdijk, W. H.; Tipping, E. Generic NICA-Donnan model parameters for metal-ion binding by humic substances. *Environ. Sci. Technol.* **2003**, *37,* 958–971.

(35) Ahrland, S.; Dahlgren, Å.; Persson, I. Stabilities and hydrolysis of some iron(III) and manganese(III) complexes with chelating ligands. *Acta Agric. Scand.* **1990**, *40,* 101–111.

(36) Burgess, J. *Ions in Solution: Basic Principles of Chemical Interactions*, chapter 7; Ellis Horwood Ltd.: Chichester, UK, 1988.

(37) Berggren Kleja, D. B.; Standring W.; Oughton, D. H.; Gustafsson, J. P.; Fifield, K.; Fraser, A. R. Assessment of isotopically exchangeable Al in soil materials using 26Al tracer. *Geochim. Cosmochim. Acta* **2005**, *69,* 5263–5277.

Received for review July 3, 2006. Revised manuscript received December 1, 2006. Accepted December 7, 2006.

ES0615730